ACES Asian Chemical Editorial Society

doi.org/10.1002/ajoc.202500288

ASIAN JOURNAL OF ORGANIC CHEMISTRY
Research Article

www.asianjoc.org

# Hydrogen-Bonded Framework With Low-Density Hexagonal Network Structure Formed by Diethynylterphenyl-Bridged Macrocyclic Hexacarboxylic Acid

Yuzuru Kanetada,[a] Ryusei Oketani,[a] Toshiyuki Sasaki,[b] Kouhei Ichiyanagi,[b] and Ichiro Hisaki*[a]

*Dedicated to the memory of Prof. Dr. Masahiko Iyoda*

Macrocyclic $\pi$-conjugated molecules are attractive building block molecules for porous molecular crystals because of their shape-persistent cyclic structures and rich electronic properties. Herein, we report a single-crystalline layered framework formed with a low-density hydrogen-bonded hexagonal network (HexNet) sheet. The sheet is composed of a $C_3$-symmetric $\pi$-conjugated building block molecule possessing a macrocyclic core expanded by diethynylterphenyl linkers and peripheral six 4-carboxyphenyl groups. The sheet has three types of vacancies, of which the largest hexagonal void has a size of 30 Å × 34 Å. The present system is the framework with the largest crystalline periodicity among the reported single-crystalline HexNet frameworks.

## 1. Introduction

Macrocyclic $\pi$-conjugated molecules have long been attractive and challenging research targets for chemists from various perspectives,[1–11] including the development of new synthetic reactions,[12–16] embodiment of the aesthetics of their exotic structures,[17–22] experimental demonstration of aromaticity and antiaromaticity of annulenes and related compounds,[23–25] and energy migration within macrocycles.[26–27] The molecules have also been applied for a building block to develop supramolecular assemblies, such as "molecular Saturn" that is a complex of a macrocycle accommodating a fullerene inside the molecular void,[28–32] one-dimensional (1D) fibers,[33–35] and two-dimensional (2D) molecular tiling on a surface.[36] The molecules and assemblies can also be converted into fascinating carbon-rich materials by transannulation cyclizations[37–41] and topochemical polymerization[42–44] thanks to the reactivity of the $\pi$-conjugated systems possessing sp-hybrid carbon atoms.

Since $\pi$-conjugated rigid macrocyclic compounds intrinsically have a pore inside the molecule due to their shape persistence, the resultant crystalline assemblies can provide inclusion spaces for guest molecules. For example, it is reported that dehydro[24]annulenes are stacked in the crystalline state to form 1D channels, in which solvent molecules are accommodated.[45] Cycloparaphenylenes give porous crystals capable of absorbing $CO_2$ gas.[46] In addition to the intrinsic pore, new vacancies can be formed by networking molecules into a low-density assembly. In recent years, porous crystals, in which molecules are accumulated by non-covalent interactions, have come into the limelight.[47] Among them, hydrogen-bonded organic frameworks (HOFs),[48–53] in which molecules are linked by intermolecular hydrogen bonding to form porous frameworks, can be constructed as designed due to directional supramolecular synthons such as a dimer of carboxylic acids.[54–56]

In 2000, Kobayashi and coworkers reported a crystal structure of hexakis(4-carboxyphenyl)benzene,[57] where the molecule successfully forms a 2D hexagonal network (HexNet) sheet through hydrogen bonding of the peripheral carboxy groups, and the sheets are further stacked without interpenetration. Later, we found that the central benzene ring of the molecule can be replaced by other $C_3$-symmetry $\pi$-conjugated skeletons,[58–60] including macrocycle ones,[61–63] to construct expanded HexNet structures via hydrogen-bonded phenylene triangle (PhT) formed by three 4,4′-dicarboxy-*o*-terphenyl (DoT) parts. As shown in Figure 1, a series of $C_3$-symmetric $\pi$-conjugated macrocycle molecules ($C_3$PI) with different ring sizes form layered HOFs with an isoreticular 2D HexNet sheet exhibiting diverse vacancies referred to as voids I, II, and III.[61–63]

[a] Y. Kanetada, Dr. R. Oketani, prof. Dr. I. Hisaki
Division of Chemistry, Graduate School of Engineering Science, The University of Osaka, 1, Osaka, Toyonaka 560-8531, Japan
E-mail: i.hisaki.es@osaka-u.ac.jp

[b] Dr. T. Sasaki, Dr. K. Ichiyanagi
Japan Synchrotron Radiation Research Institute (JASRI), 1-1-1 Kouto, Sayo-cho, Sayo-gun, Hyogo 679-5198, Japan

*[Correction added on 29 May 2025, after first online publication: The copyright line was changed.]*

*Supporting information for this article is available on the WWW under https://doi.org/10.1002/ajoc.202500288*

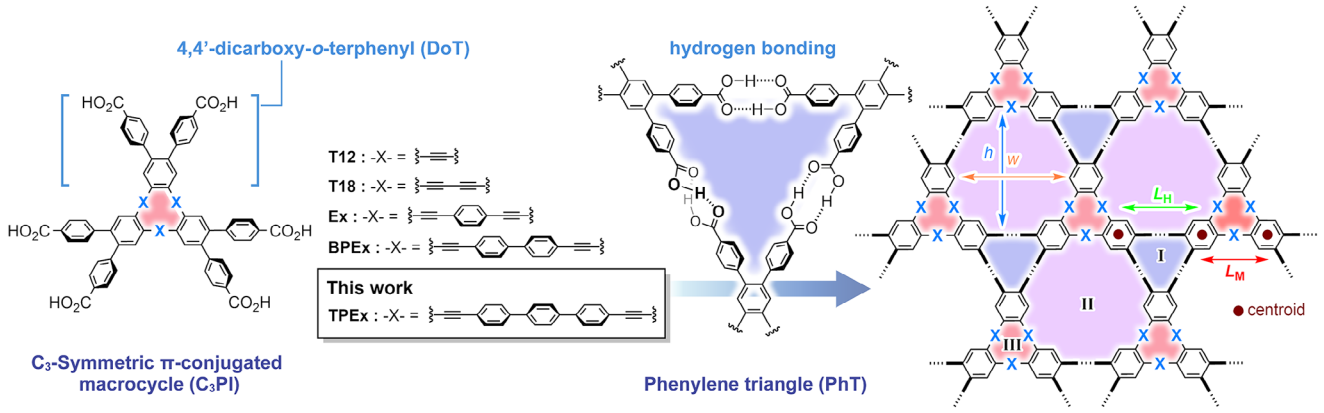


**Figure 1.** Concept of this study: Construction of porous hexagonal network (HexNet) structures from triangular macrocyclic molecules possessing 4,4′-dicarboxy *o*-terphenyl (DoT) moieties via formation of a hydrogen-bonded phenylene triangle (PhT) motif. HexNet sheet involves three types of voids (I, II, and III). Structural parameters $L_H$, $L_M$, $h$, and $w$ denote side length of the PhT motif (void I), side length of the macrocyclic core, height of the hexagonal void II, and width of the hexagonal void II. Centroids of annulated benzene rings are used for estimation of $L_H$ and $L_M$.

What we are interested in is the limitation of the size of a $C_3$PI for the formation of crystalline HexNet HOFs and how large voids can be achieved. In this paper, we report on the synthesis of expanded macrocyclic hexacarboxylic acid **TPEx** and the construction of a HexNet HOF composed of **TPEx**. In this system, it was necessary to introduce alkoxy side chains into the linker unit to increase the solvent solubility of a synthetic intermediate, in contrast to the reported systems without side chains. Despite the potential for side chains to prevent the formation of a crystalline assembly, we found that **TPEx** successfully gave single crystals of HexNet HOF **TPEx-1**. High-flux synchrotron X-ray radiation allowed the structure to be analyzed. This system is a single-crystalline, $C_3$PI-based HexNet HOF with the largest network periodicity, although other types of HOFs with significant pore size have also been reported so far.[64–68]

## 2. Results and Discussion

### 2.1. Synthesis of TPEx

Synthesis of the macrocyclic molecule **TPEx** with diethynylterpnenyl side parts was planned, as shown in Scheme 1. The molecular skeleton of **TPEx** can be constructed by cyclotrimerization of 4-[(2-ethynylphenyl)ethynyl]-4′″-iodo-1,1′:4′,1″′-terphenyl derivative **1** under a Sonogashira cross-coupling condition. Building block **1** can be synthesized by a 1:1 stoichiometric Sonogashira cross-coupling reaction between asymmetric diethynyl benzene derivative **2**, which was reported by our group,[62] and diiodoterphenyl derivative **3**. Since the solubility of **TPEx** in common organic solvents was anticipated to be lower due to its large and rigid structure, we planned to modify the linker moiety by alkoxy groups, which, on the other hand, might inhibit the crystallization of the resultant frameworks.

First, we started the synthesis of linker molecules **3** (Scheme 2). Pristine **3a** was commercially available. Linker **3b** with methoxy groups was obtained by a Suzuki–Miyaura cross-coupling reaction with 1,4-dibromo-2,5-dimethoxybenzene (**4b**) and phenylboronic acid, followed by iodination of the resultant terphenyl derivative **5b** with iodine monochloride in moderate isolated yield (Path A).[69] Similarly, an attempt was made to synthesize linker **3c** with a butoxy group from **4c** via terphenyl derivative **5c**. However, treatment of **5c** with iodine monochloride in dichloromethane solution resulted in chlorination at an *ortho*-position of the butoxy group in the central benzene ring to give **3c′** instead of the diiodinated derivative **3c**. This unexpectedly formed compound was characterized by $^1$H and $^{13}$C NMR spectroscopy and high-resolution mass spectrometry. On the other hand, bis(trimethylsilyl)terphenyl derivative **6**, which was synthesized from **4c** and (4-(trimethylsilyl)phenyl)boronic acid, was iodinated under milder condition by using iodine in the presence of silver(I) trifluoroacetate yielded diodoterphenyl derivative **3c** in moderate isolated yield (Path B).

A cross-coupling reaction of diethynyl benzene derivative **2**[62] and linker molecules **3** was carried out to prepare **1**. When the diiodoterphenyl derivative **3a** or **3b** was used in the Sonogashira cross-coupling reaction with **2**, the desired product was not obtained, probably due to the low solubility of **3a** and **3b**. On the other hand, [(2-ethynylphenyl)ethynyl]iodoterphenyl derivative **4** was obtained in good yield when three equivalents of **3c** was used for the reaction (Scheme 3). Desilylation of **4** using tetrabutylammonium fluoride, followed by cyclotrimerization of the resulted terminal acetylene **1** under a Sonogashira cross-coupling reaction condition, gave macrocyclic compound **5**. The formation of the macrocyclic structure was confirmed by $^1$H and $^{13}$C NMR spectra and high-resolution mass spectrometry. Hydrolysis of hexaester derivative **5** in the presence of potassium hydroxide yielded macrocyclic hexacarboxylic acid **TPEx**.

### 2.2. Electronic Properties

UV–vis absorption and fluorescence spectra of **TPEx** in a DMF solution were shown in Figure 2. The absorption spectrum shows two broad bands at 309 and 360 nm ascribable to $\pi$–$\pi^*$ transitions. To compare the observed absorption spectrum

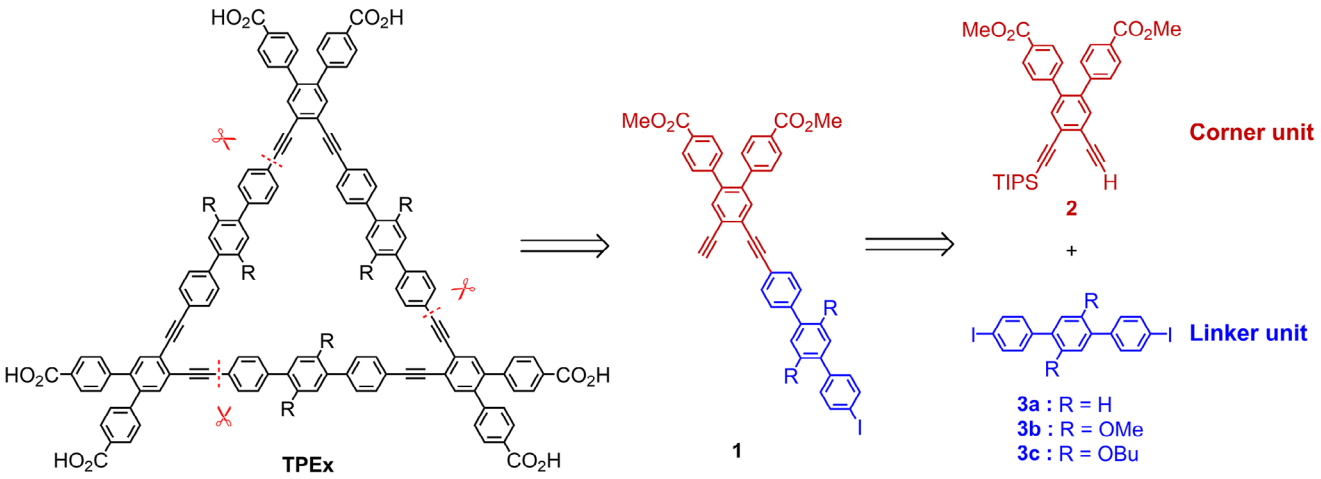


**Scheme 1.** Retrosynthesis of **TPEx**.

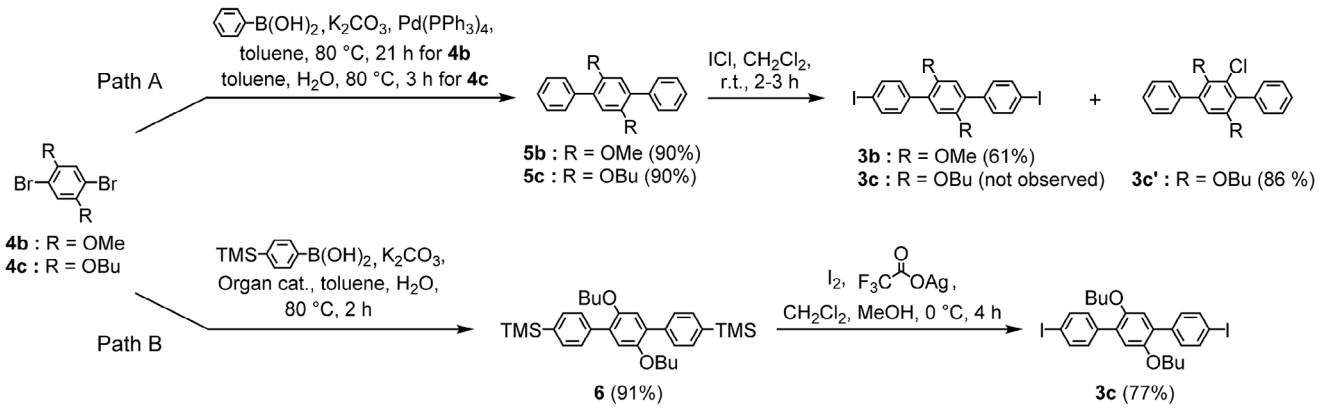


**Scheme 2.** Synthesis of linker molecules **3**. Abbreviations, TMS: trimethylsilyl.

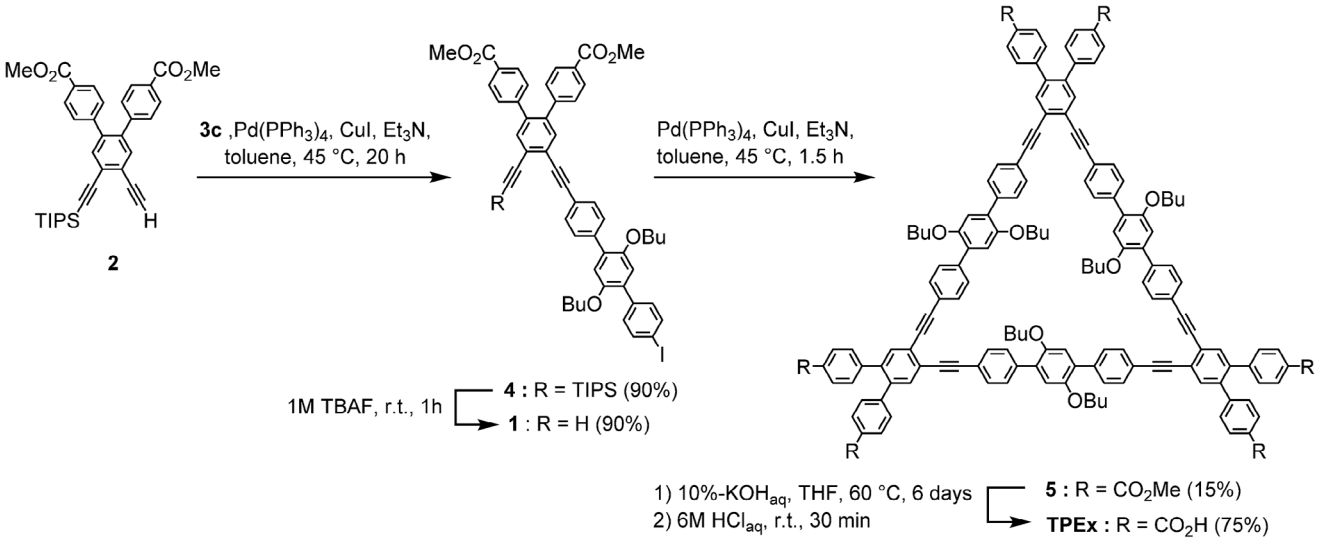


**Scheme 3.** Synthesis of macrocycle **TPEx**. Abbreviations, TBAF: tetrabutylammonium fluoride.

with the theoretical one, single-electronic transitions were calculated for a model compound that possesses methoxy groups instead of butoxy groups using the TD-DFT method. The CAM-B3LYP/6–31G** level of theory with the polarizable continuum model (PCM) was applied for the single-point calculation on the geometrically optimized structure (Figure S1). The oscillator strengths were shown with gray bars in Figure 2, which moderately agreed with the observed spectrum. The visualized

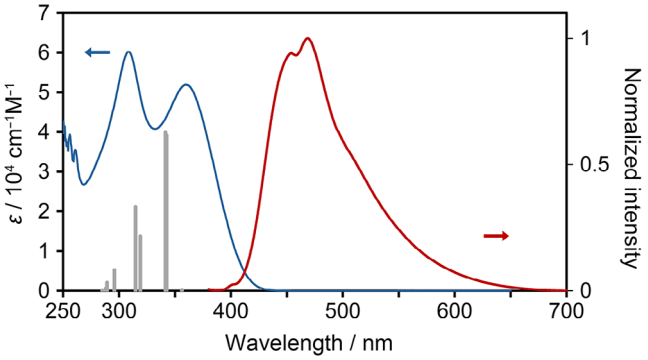


**Figure 2.** UV–vis absorption (cyan) and fluorescence (red) spectra of **TPEx** in a DMF solution. Calculated oscillator strength for electronic transitions are shown with grey bars in arbitral units.

MOs show that HOMO and neighboring occupied MOs are mainly localized on the core with nonsymmetric distribution, while LUMO and neighboring unoccupied MOs are spread and distributed from the core to the peripheral carboxyphenyl groups. Each of the oscillator sterengths involves several transition modes from/to different MOs (Figure S2). The fluorescence spectrum of **TPEx** in the DMF solution shows a less structured profile with $\lambda_{max}$ of 469 nm. The fluorescence quantum yield was determined to be 0.26.

### 2.3. Crystal Structure

To obtain an HOF, **TPEx** was recrystallized at 60 °C from a mixed solution of DMF and aromatic solvents such as methyl benzoate, 1,2-dichlorobenzene, and 1,2,4-trichlorobenzene. When methyl benzoate was applied as an aromatic solvent, relatively large crystals with a size of 75 μm × 50 μm × 30 μm suitable for single-crystal X-ray diffraction (SCXRD) analysis were obtained (Figure S3). The crystal structure of HOF **TPEx-1** was consequently revealed using a high-flux synchrotron X-ray radiation source, although the quality of the crystal data remains low because of disorder of the butoxy groups and solvent molecules (Table S1).[70] **TPEx-1** crystallized into the space group of $P2_1/c$ in the monoclinic system with a large cell: $a = 31.3306(3)$ Å, $b = 40.3919(5)$ Å, $c = 14.7910(2)$ Å, $\beta = 100.941(1)°$, and $V = 18{,}377.8$ Å$^3$. In the crystal, two peripheral carboxy phenyl groups of **TPEx** are disordered into two conformations with different twisted angles due to the following reason. Adjacent carboxyphenyl groups in the DoT moiety are restricted in the conformations that they can take due to their steric hindrance. The hydrogen-bonded PhT motif, therefore, essentially involves a conformational mismatch, namely, one of the three hydrogen-bonded dimers being frustrated.[58] Consequently, the two carboxyphenyl groups forming the frustrated dimer are disordered (Figure S4). One of three sets of the butoxy side chains is also disordered into two confirmations related by a 180° rotation of the central benzene ring in the therphenyl moiety. The root-mean-square deviation (RMSD) for the positions of the carbon atoms in the macrocycle skeleton, except for the terphenyl moieties, was calculated to be 0.298 Å against the mean plane of the macrocycle. The central benzene rings in the terphenyl moieties exhibit relatively large twisted angles of 53.8°–66.3° against the mean plane of the macrocycle. The butoxy side chains are directed up and down the macrocyclic plane and have large thermal ellipsoid.

**TPEx** molecules form a low-density HexNet sheet structure by intermolecular hydrogen bonding of the peripheral carboxy groups via the formation of the cyclic PhT motifs (Figure 3a). The butoxy groups stand upright in the vertical direction of the HexNet sheet. There are three vacancies within the HexNet sheet: (I) small triangular vacancy formed by PhT, (II) a large hexagonal vacancy, and (III) an intrinsic void of the cyclic molecule. In particular, void II has an aperture of 30 Å × 34 Å, which is the largest among ever-reported $C_3$PI-based HexNet sheets constructed in a single crystalline state. Table 1 shows structural parameters of $C_3$PI-based HexNet HOFs reported before. In all cases, the sizes of void I are the same: $L_H$ ranges 17.8–18.1 Å, while those of void II significantly depend on the cores: $L_M$, $h$, and $w$ range 6.9–22.3 Å, 18.0–33.3 Å, and 16.8–29.3 Å, respectively. The void ratio also increases as the core size increases, except for **TPEx-1**, in which the butoxy substituent groups fill the void.

Figure 3b shows the stacking pattern for four layers of a HexNet sheet. Neighboring HexNet layers that are stacked are related by an inversion operation, resulting in subdivision of large void III. The first and second layers are stacked in such a way that the overlap of the rhombic framework is large, resulting in overlapping vacancies I and III, and also vacancies II in each layer (Figure 4a). In the second and third layers, only the two opposite sides of the rhombic framework overlap in a staggered lamination (Figure 4b). This results in vacancies II being subdivided. The stacking pattern of the third and fourth layers is the same as that of the first and second layers (Figure 4c). There are three types of stacking motifs. That is, stacking between (i) a carboxyphenyl dimer and terphenyl, (ii) carboxy dimers, and (iii) carboxyphenyl dimers (Figure 4d). Overlap of the first and second (or the third and fourth) layers took place with motif (i), while that of the second and third layers took place with motif (ii) and (iii). It is already known that the mode of stacking depends on the homology between the sizes of the PhT and the $C_3$PI core.[63] If they are the same size, a large-aperture channel is formed, while if they are different, a complex channel with split apertures is formed. In the present system, the macrocycle is larger than the PhT motif, resulting in a complicated layer structure with split narrow channels along the $a$-axis (Figure S5).

This system is the first example of $C_3$PI-based HexNet HOFs in which alkoxy chains have been introduced in a molecular core. As mentioned earlier, the butoxy groups stand in the vertical direction of the HexNet sheet and penetrate into the void space of the neighboring layers. The butoxy groups are contacted by van der Waals forces. For example, the butoxy groups of the second layer penetrate into the voids I and III of the first layer (Figure 5a), and the hydrogen atom of the butoxy groups makes contact with the oxygen atoms of the carboxy groups through a weak CH/O interaction. Similarly, the butoxy groups of the macrocycle in the third layer intrude into the void III in

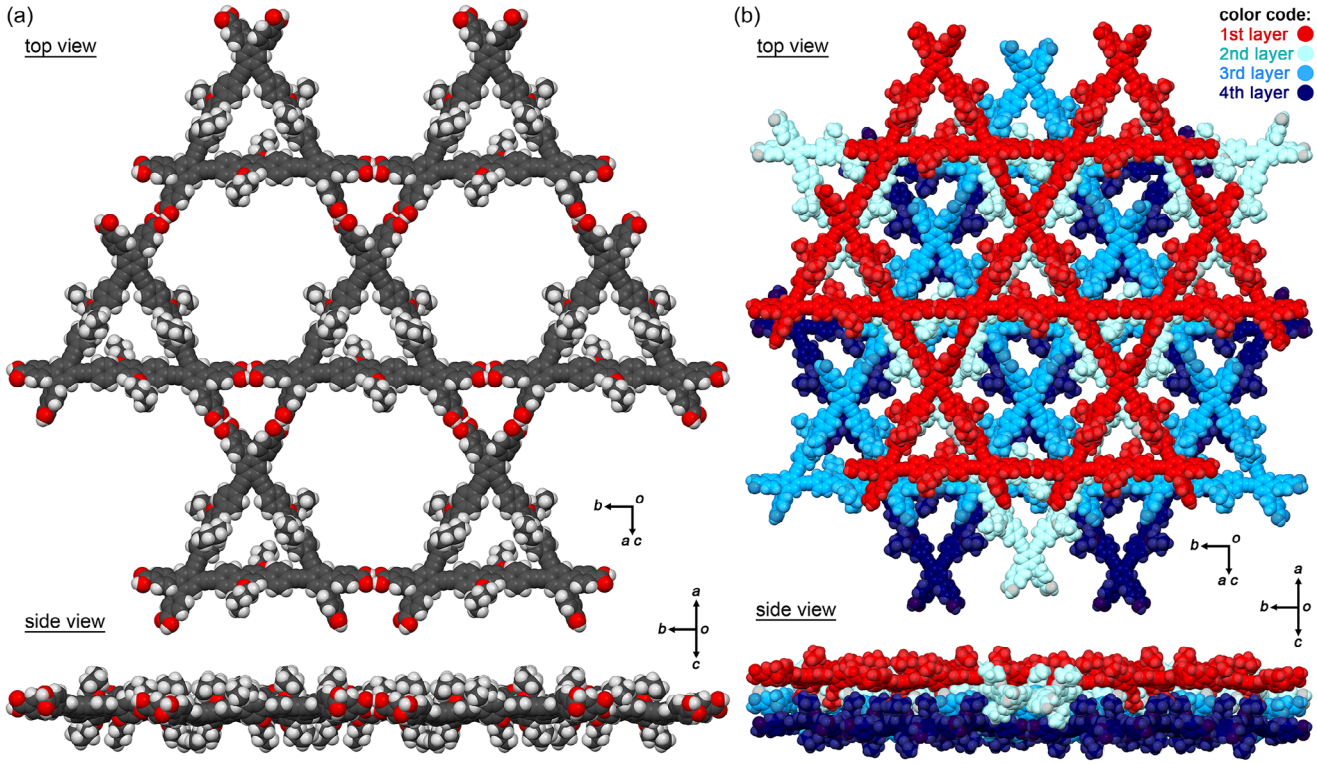


**Figure 3.** Crystal structure of **TPEx**. (a) A HexNet sheet. (b) Selected neighboring four layers of HexNet sheets.

**Table 1.** Comparison of geometrical parameters of HexNet sheets.

| | T12-1 | T18-1 | Ex-1 | BPEx-1 | TPEx-1 |
|---|---|---|---|---|---|
| $L_H$ [a] / Å | 18.07 | 18.10 | 18.10 | 17.88 | 18.06 |
| $L_M$ [b] / Å | 6.86 | 9.43 | 13.71 | 17.83 | 22.26 |
| $h$ [c] / Å | 18.0 | 20.5 | 24.8 | 28.7 | 33.3 |
| $w$ [d] / Å | 16.8 | 19.3 | 22.0 | 24.9 | 29.3 |
| Void ratio [e] | 0.41 | 0.58 | 0.59 | 0.64 | 0.40 |
| Ref. | Ref. [62] | Refs. [61, 62] | Ref. [62] | Ref. [63] | This work |

[a] Side length of hydrogen-bonded PhT motif (void I) [b] Side length of the macrocyclic core. [c] Height of the hexagonal void II. [d] Width of the hexagonal void II. [e] Void ratio of the solvent accessible volume per the unit cell calculated by PLATON software.

the second layer (Figure 5b), and the butoxy groups in both layers contact with each other, although the details are not discussed because of the highly disordered structure with large anisotropic displacement ellipsoids. Such interactions sometimes cause interpenetration of frameworks,[71] which, however, is not observed in the present system. Interactions between the solvent molecules and the HexNet framework also may affect the stacking manner of layers, although guest solvent molecules were not able to be solved crystallographically due to severe disorder.

## 3. Conclusion

Hexacarboxylic acid **TPEx** with a diethynylterphenyl-linked $C_3$-symmetric macrocycle skeleton was synthesized. The introduction of butoxy side chains into the molecule was necessary to increase the solubility of the synthetic intermediate. Crystallization of **TPEx** gave single crystals of the desired HexNet HOF, structural analysis of which was successfully accomplished using high flux synchrotron X-ray radiation. The HOF **TPEx -1** has a layered structure of 2D sheets with a hexagonal molecular network formed via hydrogen bonding of the carboxylic acids. The sheet possesses three types of vacancies, the largest of which has a hexagonal aperture of 30 Å × 34 Å. However, the adjacent sheets were stacked in an inverted manner, resulting in splitting of large vacancies. Butoxy groups penetrated into the voids of the neighboring layer, but did not prevent **TPEx** from formation of a HexNet framework. Although the total amount of material that could be synthesized in the present study was too small to assess the porosity of the bulk HOFs, it was still possible to reveal how large macrocyclic molecules can be

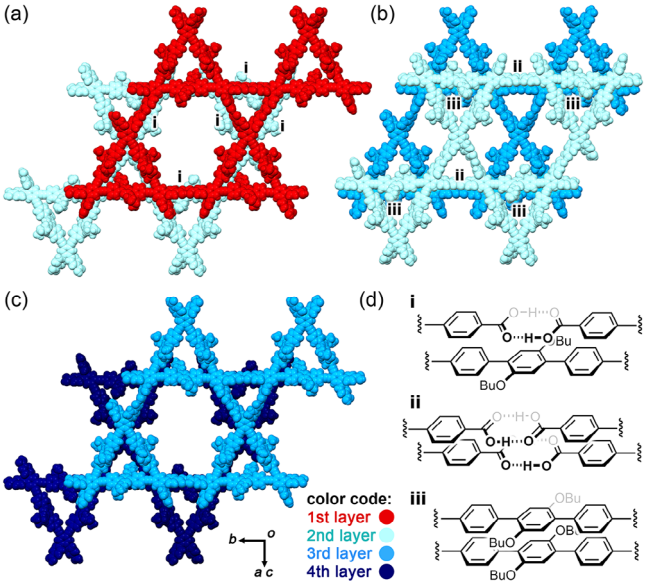


**Figure 4.** Overlap manners of the adjacent two layers of (a) first-second, (b) second-third, and (c) third-fourth layers. (d) Schematic representations of the overlapped moieties composed of (i) carboxyphenyl dimer and terphenyl, (ii) carboxy dimers, and (iii) carboxyphenyl dimers.

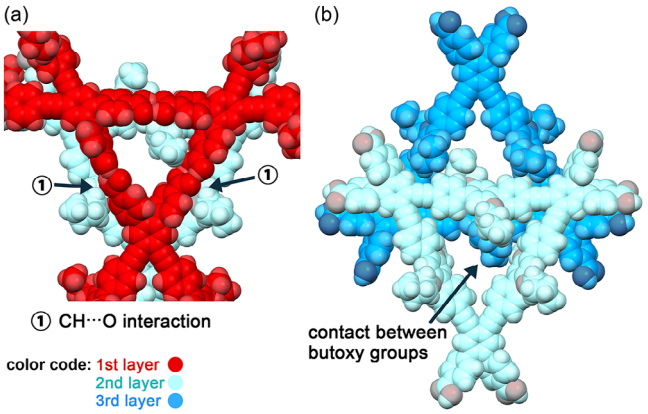


**Figure 5.** Interpenetration of the butoxy side chains into voids of the next layer for (a) first-second and (b) second-third layers.

used to form HexNet layered HOFs, and whether single crystal structural analysis can be carried out. It is likely that low density HexNet HOFs can be constructed with even larger cyclic $\pi$-conjugated molecules. The large aperture in low density HexNet HOFs may be applied for inclusion and selective separation for biomolecules such as enzymes.

## 4. Experimental Section

### 4.1. Terphenyl Derivative 5b

A mixture of 1,4-dibromo-2,5-dimethoxybenzene (4.45 g, 15.0 mmol), phenyl boronic acid (5.52 g, 45.3 mmol), $Pd(PPh_3)_4$ (752 mg, 651 µmol) in deoxygenated toluene (75 mL) and 2 M $K_2CO_3$ aqueous solution (38 mL) was stirred at 80 °C for 21 h under argon atmosphere. After the organic solvent was removed under vacuum, the residue was extracted with $CH_2Cl_2$, washed with water and brine, dried over anhydrous $MgSO_4$. The product was purified by column chromatography (silica gel, hexane/$CH_2Cl_2$ = 3/1 to 1/1 v/v) to give **5b** (3.93 g, 13.5 mmol, 90%). $^1$H NMR (400 MHz, $CDCl_3$): $\delta$ 7.61–7.57 (m, 4H), 7.47–7.43 (m, 4H), 7.37–7.33 (m, 2H), 6.98 (s, 2H), 3.79 (s, 6H) ppm.

### 4.2. Terphenyl Derivative 3b

To a solution of **5b** (3.14 g, 10.8 mmol) dissolved in $CH_2Cl_2$ (65 mL) was added iodine monochloride (2.3 mL, 43.9 mmol) under argon atmosphere. After stirred for 3 h at room temperature, saturated sodium thiosulfate (60 mL) was added. The organic layer was extracted with $CH_2Cl_2$, washed with saturated sodium thiosulfate, and dried over $MgSO_4$. The product was purified by column chromatography (silica gel, hexane/$CH_2Cl_2$ = 3/1 to 0/1 v/v) to give **3b** (3.58 g, 6.60 mmol, 61%) as white solid. $^1$H NMR (400 MHz, $CDCl_3$): $\delta$ 7.61–7.57 (m, 4H), 7.47–7.43 (m, 4H), 7.37–7.33 (m, 2H), 6.98 (s, 2H), 3.79 (s, 6H) ppm.

### 4.3. Terphenyl Derivative 5c

A mixture of **4c** (9.58 g, 25.2 mmol), phenylboronic acid (9.52 g, 75.9 mmol), $Pd(PPh_3)_4$ (1.70 g, 1.47 mmol), $K_2CO_3$ (17.3 g, 125 mmol) in deoxygenated toluene (150 mL) and water (80 mL) was stirred at 80 °C for 3 h. The product was extracted with $CH_2Cl_2$, washed with water and brine, dried over anhydrous $MgSO_4$, and recrystallized from EtOH/MeOH to give **5c** (5.00 g, 12.9 mmol, 51%) as a yellow solid. Mp 96 °C. $^1$H NMR (400 MHz, $CDCl_3$): $\delta$ 7.62–7.58 (m, 4H), 7.45–7.39 (m 4H), 7.33 (tt, $J$ = 7.1 and 2.0 Hz, 2H), 6.99 (s, 2H), 3.91 (t, $J$ = 6.4 Hz,4H), 1.67 (quin, $J$ = 6.4 Hz, 4H), 1.39 (sext, $J$ = 7.5 Hz, 4H), 0.89 (t, $J$ = 7.4 Hz, 6H) ppm. $^{13}$C NMR (100 MHz, $CDCl_3$): $\delta$ 150.5, 138.6, 131.1, 129.7, 128.1, 127.0, 116.6, 69.5, 31.6, 19.4, 13.9 ppm. HR-MS (FAB) calcd. for $C_{26}H_{30}O_2$ $[M]^+$: 374.2246; found: 374.2249.

### 4.4. Bis(trimethylsilyl)Terphenyl Derivative 6

A mixture of potassium carbonate (186 mg, 1.34 mmol), **4c** (102 mg, 268 µmol), 4-(trimethylsilyl)phenylboronic acid (152 mg, 783 µmol), and Organ's catalyst (5.74 mg, 8.44 µmol) in toluene (6.0 mL) and water (3.0 mL) was refluxed at 80 °C for 2 h under argon atmosphere. The product was extracted with $CH_2Cl_2$, washed with water and brine, dried over anhydrous $MgSO_4$, and purified by column chromatography (silica gel, hexane/$CH_2Cl_2$ = 1/19 to 1/0 v/v) to give **6** (126 mg, 242 µmol, 91%) as a white solid. Mp 150 °C. $^1$H NMR (400 MHz, $CDCl_3$): $\delta$ 7.63–7.55 (m, 8H), 6.99 (s, 2H), 3,91 (t, $J$ = 6.5 Hz, 4H), 1.68 (quin, $J$ = 7.9 Hz, 4H), 1.39 (sext, $J$ = 7.5 Hz, 4H), 0.89 (t, $J$ = 7.4 Hz, 6H), 0.31 (s, 18H) ppm. $^{13}$C NMR (100 MHz, $CDCl_3$): $\delta$ 150.5, 139.0, 139.0, 133.1, 130.9, 128.9, 116.5, 69.5, 31.6, 19.4, 13.9, −0.9 ppm. HR-MS (FAB) calcd. for $C_{32}H_{46}O_2Si_2$ $[M]^+$: 518.3036, found: 518.3032.

### 4.5. Formation of Monochlorinated Terphenyl Derivative 3c'

To a solution of **5c** (600 mg, 1.60 mmol) dissolved in anhydrous $CH_2Cl_2$ (12 mL) was added dropwise 0.51 M iodine monochloride in anhydrous $CH_2Cl_2$ (7.3 mL, 3.72 mmol) at room temperature. The reaction mixture was stirred for 2 h at room temperature and quenched with water. The organic layer was extracted with $CH_2Cl_2$, washed with aqueous $Na_2S_2O_3$ and brine, and dried over anhydrous $MgSO_4$. The product was purified by column chromatography (silica gel, hexane/$CH_2Cl_2$ = 8/2 v/v) to give monochlorinated terphenyl derivative **3c'** (561 mg, 1.37 mmol, 86%) as pale yellow solid. M.p. 63 °C. $^1$H NMR (400 MHz, $CDCl_3$): $\delta$ 7.64–7.60 (m, 2H), 7.47–7.40 (m, 4H), 7.40–7.35 (m, 2H), 7.35–7.31 (m, 2H), 6.86 (s, 1H), 3.87 (t, $J$ = 6.4 Hz, 2H), 3.56 (t, $J$ = 6.4 Hz, 2H), 1.59–1.44 (m, 4H), 1.31–1.19 (m, 4H), 0.82 (t, $J$ = 7.4 Hz, 3H), 0.77 (t, $J$ = 7.4 Hz, 3H) ppm. $^{13}$C NMR (100 MHz,

$CDCl_3$): $\delta$ 153.3, 146.9, 138.3, 135.8, 135.8, 131.0 130.6, 129.4, 129.2, 128.3, 127.8, 127.7, 127.4, 113.4, 73.3, 69.2, 32.2, 31.3, 19.2, 19.1, 13.8, and 13.8 ppm. HR-MS (FAB) calcd. for $C_{26}H_{29}ClO_2$ $[M]^+$: 408.1856., found: 408.1845.

### 4.6. Diiodoterphenyl Derivative 3c

To a solution of **6** (5.23 g, 10.0 mmol) dissolved in anhydrous $CH_2Cl_2$ (262 mL) and methanol (240 mL) was added silver trifluoroacetate (9.33 g, 42.2 mmol) under argon atmosphere, and the reaction vessel was cooled by an ice bath. After the solute had completely dissolved, iodine (7.67 g, 30.2 mmol) was added. The reaction mixture was stirred at 0 °C for 4 h. The reaction mixture was filtrated, and a sodium thiosulfate aqueous solution was added to the filtrate. The mixture was extracted with $CH_2Cl_2$, washed with sodium thiosulfate aqueous solution, dried over magnesium sulfate. The crude product was recrystallized from hexane to give **3c** as a white solid (4.79 g, 7.65 mmol, 77%). M.p. 127 °C. $^1$H NMR (400 MHz, $CDCl_3$): $\delta$ 7.77–7.72 (m, 4H), 7.36–7.31 (m, 4H), 6.92 (s, 2H), 3.90 (t, $J$ = 6.5 Hz, 4H), 1.67 (quin, $J$ = 6.4 Hz, 4H), 0.90 (t, $J$ = 7.4 Hz, 6H) ppm. $^{13}$C NMR (100 MHz, $CDCl_3$): $\delta$ 150.3, 138.0, 137.2, 131.5, 130.1, 116.0, 92.9, 69.5, 31.5, 19.4, and 13.9 ppm. HR-MS (FAB) calcd. for $C_{26}H_{28}I_2O_2$ $[M]^+$: 626.0179, found: 626.0189.

### 4.7. (2-Ethynylphenyl)ethynyl)-iodoterphenyl Derivative 4

To a mixture of **3c** (342 mg, 546 µmol), CuI (8.04 mg, 42.2 µmol), and $Pd(PPh_3)_4$, (12.9 mg, 11.2 µmol) in deoxygenated toluene (5.0 mL) and $Et_3N$ (3.0 mL) was added a solution of **2** (100 mg, 182 µmol) dissolved in degassed toluene (8.0 mL). The reaction mixture was stirred at 45 °C for 20 h. After solvent was removed under vacuum, the resulting mixture was extracted with $CH_2Cl_2$, washed with water and brine, dried over anhydrous $MgSO_4$. The product was purified by column chromatography (silica gel, hexane/$CH_2Cl_2$ = 2/1 v/v) to give **4** (171 mg, 163 µmol, 90%) as a yellow solid. Mp. 104 °C. $^1$H NMR (400 MHz, $CDCl_3$): $\delta$ 7.90 (dd, $J$ = 8.4, 1.9 Hz, 4H), 7.75 (d, $J$ = 8.4 Hz, 2H), 7.68–7.57 (m, 6H), 7.37–7.35 (m, 1H), 7.35–7.33 (m, 1H), 7.22–7.18 (m, 4H), 6.99 (s, 1H), 6.94 (s, 1H), 3.94 (t, $J$ = 6.6, 6H), 3.91 (s, 6H), 1.67 (quin, $J$ = 6.4 Hz, 4H), 1.41 (sextd, $J$ = 2.8 and 7.5 Hz, 4H), 0.91 (td, $J$ = 7.4 Hz, 2.0, 6H) ppm. $^{13}$C NMR (100 MHz, $CDCl_3$): $\delta$ 166.9, 150.6, 150.4, 144.6, 139.6, 139.4, 138.8, 138.0, 137.2, 134.9, 134.3, 131.6, 130.6, 130.1, 129.9, 129.8, 129.6, 129.5, 129.1, 126.1, 125.7, 121.7, 116.2, 116.1, 104.9, 96.7, 94.6, 92.9, 88.2, 69.5, 52.3, 31.6, 31.6, 19.4, 18.9, 18.8, 13.9, and 11.5 ppm. HR-MS (FAB) calcd. for $C_{61}H_{65}IO_6Si$ $[M]^+$: 1048.3595; found, 1048.3592.

### 4.8. Terminal Acetylene 1

To a solution of **4** (219 mg, 209 µmol) dissolved in degassed THF (10 mL) was added 1 M solution of tetrabutylammonium fluoride in THF (2.5 mL) under argon atmosphere. After stirring at room temperature for 1 h, the reaction mixture was quenched with water (10 mL), extracted with $CHCl_3$, washed with water, and brine, dried over anhydrous $MgSO_4$. The product was purified by column chromatography (silica gel, hexane/ethyl acetate = 2/1 v/v) to give **1** (167 mg, 187 µmol, 90%) as a brown solid. Mp 74 °C. $^1$H NMR (400 MHz, $CDCl_3$): $\delta$ 7.96–7.86 (m, 4H), 7.75 (d, $J$ = 8.1 Hz, 2H), 7.68–7.58 (m, 6H), 7.36 (s, 1H), 7.34 (s, 1H), 7.23–7.17 (m, 4H), 6.98 (s, 1H), 6.94 (s, 1H), 3.94 (s, 1H), 3.91 (s, 6H), 3.96–3.90 (m, 4H), 1.67 (quin, $J$ = 7.54 Hz, 4H), 1.41 (sext, $J$ = 7.4 Hz, 4H), 0.91 (t, $J$ = 7.4 Hz, 6H) ppm. $^{13}$C NMR (100 MHz, $CDCl_3$): $\delta$ 166.9, 150.5, 150.4, 144.5, 144.4, 140.1, 139.4, 138.0, 137.2, 134.8, 133.9, 131.6, 131.5, 130.5, 130.2, 129.8, 129.7, 129.2, 129.2, 126.4, 124.6, 121.6, 116.1, 95.1, 92.9, 87.8, 82.2, 81.8, 69.5, 69.5, 52.3, 31.6, 31.6, 29.9, 19.4, 18.0, 17.9, 17.8, 17.8, 17.4, 13.9, 12.9, 12.5, 1.77, 1.15 ppm. HR-MS (FAB) calcd. for $C_{52}H_{45}IO_6$ $[M]^+$: 892.2261; found: 892.2252.

### 4.9. Macrocyclic Hexaester 5

A mixture of **1** (402 mg, 450 µmol), CuI (44.2 mg, 232 µmol), and $Pd(PPh_3)_4$ (57.8 mg, 50.0 µmol) in deoxygenated toluene (42 mL) and $Et_3N$ (20 mL) was stirred at 40 °C for 1.5 h. After the solvent was removed under vacuum, the reaction mixture was extracted with $CHCl_3$, washed with water and brine, dried over anhydrous $MgSO_4$. The product was purified by column chromatography (silica gel, $CH_2Cl_2$/$CHCl_3$ = 10/0 to 7/3 v/v), followed by recycling HPLC to give macrocycle **5** (50.8 mg, 22.1 µmol, 15%). Mp > 300 °C. $^1$H NMR (400 MHz, $CDCl_3$): $\delta$ 7.93 (d, $J$ = 8.4 Hz, 4H), 7.73–7.61 (m, 10H), 7.24 (d, $J$ = 8.4 Hz, 4H), 7.02 (s, 1H), 3.95 (t, $J$ = 6.4 Hz, 4H), 3.92 (s, 6H), 1.69 (quin, $J$ = 6.2 Hz, 1H), 1.41 (sext, $J$ = 7.4 Hz, 4H), 0.89 (t, $J$ = 7.4 Hz, 6H) ppm. $^{13}$C NMR (100 MHz, $CDCl_3$): $\delta$ 166.9, 150.6, 144.6, 139.4, 138.9, 133.8, 131.4, 130.6, 129.8, 129.7, 129.6, 129.1, 125.9, 121.8, 116.2, 95.0, 88.3, 69.5, 52.2, 31.0, 19.4, and 13.9 ppm. HR-MS (MALDI) calcd. for $C_{156}H_{132}O_{18}$ $[M]^+$: 2292.9414, found: 2292.9408.

### 4.10. Hexacarboxylic Acid TPEx

A mixture of **5** (48.1 mg, 21.0 µmol), 10% $KOH_{aq}$ (14 mL), and THF (17 mL) was stirred at 60 °C for 6 days. After THF was removed under vacuum, the residue solid was collected by filtration. The solid was dispersed in water and treated with 6 M $HCl_{aq}$ until the pH reached 1. After letting the suspension sit for 30 min, the precipitate was filtered, washed with water (30 mL) and $CHCl_3$ (30 mL), and dried in vacuum condition to give **TPEx** (34.6 mg, 15.7 µmol 75%) as a pale yellow solid. Mp > 300 °C. $^1$H NMR (400 MHz, $CDCl_3$): $\delta$ 13.5 (s, 2H), 8.16 (d, $J$ = 8.28, 4H), 8.07–7.99 (m, 10H), 7.63 (d, $J$ = 8.24 Hz, 4H), 7.46 (s, 2H,), 4.31 (t, $J$ = 6.28 Hz, 4H), 1.91 (quin, $J$ = 6.24 Hz, 4H), 1.64 (sext, $J$ = 7.56 Hz, 4H) 1.09 (t, $J$ = 7.36 Hz, 4H) ppm. $^{13}$C NMR (100 MHz, $CDCl_3$): $\delta$ 167.1, 162.4, 150.4, 144.2, 140.1, 139.2, 131.29, 130.2, 130.1, 130.1, 130.0, 129.4, 125.2, 121.2, 115.8, 94.7, 88.1, 68.9, 31.4, 19.2, and 13.3 ppm. HR-MS (MALDI) calcd. for $C_{150}H_{120}O_{18}$ $[M]^+$: 2208.8474; found:2208.8469.

## Acknowledgments

This work was supported by KAKENHI (JP22K05054, JP23H04029, and JP24K01468) from JSPS and MEXT Japan, I. H. thanks Hoansha Foundation, Iketani Science and Technology Foundation for their financial support. The authors thank the Cybermedia Center, The University of Osaka, for use of the Super-computer for Quest to Unsolved Interdisciplinary Datascience (SQUID). The authors acknowledge Ms. R. Miyake at The University of Osaka for HR-MS analysis, Dr. R. Matsuoka and Prof. Dr. T. Kusamoto at The University of Osaka for fluorescence quantum yield determination. Synchrotron X-ray diffraction data were collected at BL40XU and BL41XU at SPring-8 with approval of the Japan Synchrotron Radiation Research Institute (JASRI, proposal Nos. 2024A1208 and 2024B1142)

## Conflict of Interest

The authors declare no conflicts of interest.

## Data Availability Statement

The data that support the findings of this study are available in the supplementary material of this article.

**Keywords:** Crystal engineering · Hexagonal · Hydrogen-bonded framework · Macrocycle · Π-conjugated

[1] S. Höger, *J. Poly. Sci.: Part A Poly. Chem.* **1999**, *37*, 2685–2698.
[2] U. H. F. Bunz, Y. Rubin, Y. Tobe, *Chem. Soc. Rev.* **1999**, *28*, 107–119.
[3] M. B. Nielsen, F. Diederich, *Chem. Rev.* **2005**, *105*, 1837–1867.
[4] I. Hisaki, M. Sonoda, Y. Tobe, *Eur. J. Org. Chem.* **2006**, 833–847.
[5] W. Zhang, J. S. Moore, *Angew. Chem., Int. Ed.* **2006**, *45*, 4416–4439.
[6] K. Tahara, Y. Tobe, *Chem. Rev.* **2006**, *106*, 5274–5290.
[7] E. J. Spitler, C. A. Johnson II, M. M. Haley, *Chem. Rev.* **2006**, *106*, 5344–5386.
[8] M. Iyoda, J. Yamakawa, M. J. Rahman, *Angew. Chem., Int. Ed.* **2011**, *50*, 10522–10553.
[9] M. Iyoda, H. Shimizu, *Chem. Soc. Rev.* **2015**, *44*, 6411–6424.
[10] K. Miki, K. Ohe, *Chem. - Eur. J.* **2020**, *26*, 2529–2575.
[11] Y. Segawa, *Bull. Chem. Soc. Jpn.* **2022**, *95*, 1600–1610.
[12] M. Iyoda, *Adv. Synth. Catal.* **2009**, *351*, 984–998.
[13] S. Yamago, Y. Watanabe, T. Iwamoto, *Angew. Chem., Int. Ed.* **2010**, *49*, 757–759.
[14] T. Nishiuchi, X. Feng, V. Enkelmann, M. Wagner, K. Müllen, *Chem. - Eur. J.* **2012**, *18*, 16621–16625.
[15] Y. Tsuchido, R. Abe, T. Ide, K. Osakada, *Angew. Chem., Int. Ed.* **2020**, *59*, 22928–22932.
[16] Y. Segawa, T. Watanabe, K. Yamanoue, M. Kuwayama, K. Watanabe, J. Pirillo, Y. Hijikata, K. Itami, *Nat. Synthesis* **2022**, *1*, 535–541.
[17] D. Ajami, O. Oeckler, A. Simon, R. Herges, *Nature* **2003**, *426*, 819–821.
[18] Z. S. Yoon, A. Osuka, D. Kim, *Nat. Chem.* **2009**, *1*, 113–122.
[19] S. Kato, N. Takahashi, Y. Nakamura, *J. Org. Chem.* **2013**, *78*, 7658–7663.
[20] T. Tanaka, A. Okuka, *Chem. Rev.* **2017**, *117*, 258–2640.
[21] Y. Segawa, D. R. Levine, K. Itami, *Acc. Chem. Res.* **2019**, *10*, 2760–2767.
[22] W. Stawsky, H. L. Anderson, *Chem. Sci.* **2024**, *15*, 16938–16946.
[23] F. Diederich, H. A. Staab, *Angew. Chem., Int. Ed. Engl.* **1978** *17*, 372–374.
[24] M. Nakagawa, *Angew. Chem.* **1979**, *91*, 215–226.
[25] R. Nozawa, J. Kim, J. Oh, A. Lamping, Y. Wang, S. Shimizu, I. Hisaki, T. Kowalczyk, H. Fliegl, D. Kim, H. Shinokubo, *Nat. Commun.* **2019**, *10*, 3576.
[26] F. Schlosser, J. Sung, P. Kim, D. Kim, F. Würthner,*Chem. Sci.* **2012**,*3*, 2778–2785.
[27] T. Kuwabara, J. Orii, Y. Segawa, K. Itami, *Angew. Chem., Int. Ed.* **2015**, *54*, 9646–9649.
[28] T. Kawase, K. Tanaka, Y. Seirai, N. Shiono, M. Oda, *Angew. Chem., Int. Ed.* **2003**, *42*, 5597–5600.
[29] J. Xia, J. W. Bacon, R. Jasti, *Chem. Sci.* **2012**, *3*, 3018–3021.
[30] T. Iwamoto, Y. Watanabe, H. Takaya, T. Haino, N. Yasuda, S. Yamago, *Chem. - Eur. J.* **2013**, *19*, 14061–14068.
[31] S. Sato, T. Yamasaki, H. Isobe, *Proc. Natl. Acad. Sci. USA* **2014**, *111*, 8374–8379.
[32] Y. Yamamoto, E. Tsurumaki, K. Wakamatsu, S. Toyota, *Angew. Chem., Int. Ed.* **2018**, *57*, 8199–8202.
[33] Y. Tobe, N. Utsumi, K. Kawabata, A. Nagano, K. Adachi, S. Araki, M. Sonoda, K. Hirose, K. Naemura, *J. Am. Chem. Soc.* **2002**, *124*, 5350–5364.
[34] L. Zang, Y. Che, J. S. Moore, *Acc. Chem. Res.* **2008**, *41*, 1596–1608.
[35] M. J. Rahman, H. Shimizu, Y. Araki, H. Ikeda, M. Iyoda, *Chem. Commun.* **2013**, *49*, 9251–9253.
[36] Y. Tobe, K. Tahara, S. De Feyter, *Bull. Chem. Soc. Jpn.* **2016**, *89*, 1277–1306.
[37] A. Fukazawa, H. Oshima, Y. Shiota, S. Takahashi, K. Yoshizawa, S. Yamaguchi, *J. Am. Chem. Soc.* **2013**, *135*, 1731–1734.
[38] A. keno, M. Hayakawa, M. Sakai, Y. Tsutsui, S. Nakatsuka, S. Seki, T. Hatakeyama, *J. Am. Chem. Soc.* **2024**, *146*, 17084–17093.
[39] S. Nobusue, A. Shimizu, K. Hori, I. Hisaki, M. Miyata, Y. Tobe, *Angew. Chem., Int. Ed.* **2013**, *52*, 4184–4188.
[40] R. Boese, A. J. Matzger, K. P. C. Vollhardt, *J. Am. Chem. Soc.* **1997**, *119*, 2052–2053.
[41] Y. Tobe, N. Nakagawa, K. Naemura, T. Wakabayashi, T. Shida, Y. Achiba, *J. Am. Chem. Soc.* **1998**, *120*, 4544–4545.
[42] K. P. Baldwin, A. J. Matzger, D. A. Scheiman, C. A. Tessier, K. P. C. Vollhardt, W. J. Youngs, *Synlett* **1995**, 1215–1218.
[43] S. Rondeau-Gagné, J. RoméoNéabo, M. Desroches, I. Levesque, M. Daigle, K. Cantin, J.-F. Morin, *Chem. Commun.* **2013**, *49*, 9546–9548.
[44] A. Lapini, S. Fanetti, M. Citroni, R. Bini, C.-O. Gilbert, S. Rondeau-Gagné, J.-F. Morin, *J. Phys. Chem. C* **2018**, *122*, 20034–20039.
[45] M. Suzuki, J. F. K. Kotyk, S. I. Khan, Y. Rubin, *J. Am. Chem. Soc.* **2016**, *138*, 5939–5956.
[46] H. Sakamoto, T. Fujimori, X. Li, K. Kaneko, K. Kan, N. Ozaki, Y. Hijikata, S. Irle, K. Itami, *Chem. Sci.* **2016**, *7*, 4204–4210.
[47] W. Yang, A. Greenaway, X. Lin, R. Matsuda, A. J. Blake, C. Wilson, W. Lewis, P. Hubberstey, S. Kitagawa, N. R. Champness, M. Schröder, *J. Am. Chem. Soc.* **2010**, *132*, 14457–14469.
[48] R.-B. Lin, Y. He, P. Li, H. Wang, W. Zhou, B. Chen, *Soc. Rev.* **2019**, *48*, 1362–1389.
[49] I. Hisaki, C. Xin, K. Takahashi, T. Nakamura, *Angew. Chem., Int. Ed.* **2019**, *58*, 11160–11170.
[50] B. Wang, R.-B. Lin, Z. Zhang, S. Xiang, B. Chen, *J. Am. Chem. Soc.* **2020**, *142*, 14399–14416.
[51] X. Song, Y. Wang, C. Wang, D. Wang, G. Zhuang, K. O. Kirlikovali, P. Li, O. K. Farha, *J. Am. Chem. Soc.* **2022**, *144*, 10663–10687.
[52] P. Li, M. R. Ryder, J. F. Stoddart, *Acc. Mater. Res.* **2020**, *1*, 77–87.
[53] H. Liaquat, M. Imran, Z. Saddique, S. Latif, K. M. Al-Ahmary, A. Sohail, H. Raza, M. Ahmedx, *J. Mol. Struct.* **2025**, *1312*, 140221.
[54] I. Hisaki, *J. Incl. Phenom. Macro. Chem.* **2020**, *96*, 215–231.
[55] Y. Suzuki, I. Hisaki, *Polym. J.* **2024**, *56*, 1–16.
[56] I. Hisaki, T. Fujii, R. Oketani, *Chem. Phys. Rev.* **2024**, *5*, 041304.
[57] K. Kobayashi, T. Shirasaka, E. Horn, N. Furukawa, *Tetrahedron Lett.* **2000**, *41*, 89–93.
[58] I. Hisaki, N. Ikenaka, N. Tohnai, M. Miyata, *Chem. Commun.* **2016**, *52*, 300–303.
[59] I. Hisaki, S. Nakagawa, H. Sato, N. Tohnai, *Chem. Commun.* **2016**, *52*, 9781–9784.
[60] I. Hisaki, Y. Suzuki, E. Gomez, Q. Ji, N. Tohnai, T. Nakamura, A. Douhal, *J. Am. Chem. Soc.* **2019**, *141*, 2111–2121.
[61] I. Hisaki, S. Nakagawa, N. Tohnai, M. Miyata, *Angew. Chem., Int. Ed.* **2015**, *54*, 3008–3012.
[62] I. Hisaki, S. Nakagawa, N. Ikenaka, Y. Imamura, M. Katouda, M. Tashiro, H. Tsuchida, T. Ogoshi, H. Sato, N. Tohnai, M. Miyata, *J. Am. Chem. Soc.* **2016**, *138*, 6617–6628.
[63] H. Yoshimura, R. Oketani, M. Naruoka, N. Tohnai, I. Hisaki, *Precis. Chem.* **2024**, *2*, 221–228.
[64] M. Mastalerz, I. Oppel, *Angew. Chem., Int. Ed.* **2012**, *51*, 5252–5255.
[65] A. Pulido, L. Chen, T. Kaczorowski, D. Holden, M. A. Little, S. Y. Chong, B. Slater, D. P. McMahon, B. Bonillo, C. J. Stackhouse, A. Stephenson, C. M. Kane, R. Clowes, T. Hasell, A. I. Cooper, G. M. Day, *Nature* **2017**, *543*, 657–666.
[66] M. I. Hashim, H. T. M. Le, T.-H. Chen, Y.-S. Chen, O. Daugulis, C.-W. Hsu, A. J. Jacobson, W. Kaveevivitchai, X. Liang, T. Makarenko, O. Š. Miljanić, I. Popovs, H. V. Tran, X. Wang, C.-H. Wu, J. I. Wu, *J. Am. Chem. Soc.* **2018**, *140*, 6014–6026.
[67] Y. Suzuki, M. Gutiérrez, S. Tanaka, E. Gomez, N. Tohnai, N. Yasuda, N. Matubayasi, A. Douhal, I. Hisaki, *Chem. Sci.* **2021**, *12*, 9607–9618.
[68] M. Yamaguchi, M. d. l. H. Tomás, A. Fujiwara, R. Oketani, K. Okubo, K. Oka, N. Tohnai, A. Douhal, I. Hisaki, *Bull. Chem. Soc. J.* **2024**, *97*, uoae004.
[69] K. Nakabayashi, T. Higashihara, M. Ueda, *Macromol.* **2011**, *44*, 1603–1609.
[70] Deposition number 2427630 (for **TpEx-1**) contains the supplementary crystallographic data for this paper. These data are provided free of charge by the joint Cambridge Crystallographic Data Centre and Fachinformationszentrum Karlsruhe Access Structures service.
[71] B. P. Benke, T. Kirschbaum, J. Graf, J. H. Gross, M. Mastalerz, *Nat. Chem.* **2023**, *15*, 413–423.

Manuscript received: March 6, 2025
Revised manuscript received: March 29, 2025
Version of record online: April 26, 2025